Available online at www.sciencedirect.com
SCIENCE DIRECT
Biochimica et Biophysica Acta 1718 (2005) 1 – 21
BIOCHIMICA ET BIOPHYSICA ACTA
BBA
http://www.elsevier.com/locate/bba

Behaviour of small solutes and large drugs in a lipid bilayer from computer simulations

D. Bemporad[a], C. Luttmann[b], J.W. Essex[a,*]

[a]School of Chemistry, University of Southampton, Highfield, Southampton, SO17 1BJ, UK
[b]Aventis Pharma S.A., 13 quai Jules Guesde, F-94403 Vitry sur Seine cedex, France

Received 2 August 2004; received in revised form 14 July 2005; accepted 14 July 2005
Available online 9 August 2005

Abstract

To reach their biological target, drugs have to cross cell membranes, and understanding passive membrane permeation is therefore crucial for rational drug design. Molecular dynamics simulations offer a powerful way of studying permeation at the single molecule level. Starting from a computer model proven to be able to reproduce the physical properties of a biological membrane, the behaviour of small solutes and large drugs in a lipid bilayer has been studied. Analysis of dihedral angles shows that a few nanosesconds are sufficient for the simulations to converge towards common values for those angles, even if the starting structures belong to different conformations. Results clearly show that, despite their difference in size, small solutes and large drugs tend to lie parallel to the bilayer normal and that, when moving from water solution into biomembranes, permeants lose degrees of freedom. This explains the experimental observation that partitioning and permeation are highly affected by entropic effects and are size-dependent. Tilted orientations, however, occur when they make possible the formation of hydrogen bonds. This helps to understand the reason why hydrogen bonding possibilities are an important parameter in cruder approaches which predict drug absorption after administration. Interestingly, hydration is found to occur even in the membrane core, which is usually considered an almost hydrophobic region. Simulations suggest the possibility for highly polar compounds like acetic acid to cross biological membranes while hydrated. These simulations prove useful for drug design in rationalising experimental observations and predicting solute behaviour in biomembranes.

Keywords: Molecular dynamics simulation; Constraint; β-blockers; DPPC membrane; Permeability

1. Introduction

For most of the routes of administration, cell membrane permeation is required for a drug molecule to reach the general circulation. Even after direct injection or even if the drug can permeate via the paracellular route in the extracellular space, it soon encounters cell membranes to be crossed in order to reach its biological target which is usually represented by a protein inside the cell cytoplasm. Most drugs cross cell membranes by passive permeation without the help of protein carriers, unless they are analogues of physiological substrates. An understanding of solute behaviour inside biological membranes is then crucial for subcellular pharmacokinetics and rational drug design [1].

Functional cell membranes are fluid mosaics of proteins within a lipid bilayer matrix [2]. Experimental and theoretical models for biological membranes, especially when studying solute permeation, are therefore phospholipid bilayers. Among them, extensive data have been collected for the dipalmitoylphosphatidylcholine (DPPC) bilayer. Recently, several ns-long all-atom MD simulations have been performed in our laboratory [3,4] investigating the permeation process of eight small organic compounds in a DPPC membrane. The eight solutes represent the most common chemical functional groups: acetamide, acetic acid, benzene, ethane, methanol, methylacetate, methyla-

* Corresponding author. Tel.: +44 23 8059 2794; fax: +44 23 8059 3781.
E-mail address: jwe1@soton.ac.uk (J.W. Essex).

0005-2736/$ - see front matter © 2005 Elsevier B.V. All rights reserved.
doi:10.1016/j.bbamem.2005.07.009

mine, water. Simulation results show in general a good correlation between the free energy in the centre of the membrane with the experimental free energy of partitioning for the solutes between water and hexadecane. The notable exception to this rule is for benzene, which, because of its size, is sensitive to the lateral packing in the lipid bilayers, supporting the view that biomembranes do not always behave like bulk solvents. With the exception of water, the diffusion coefficients of the molecules are broadly similar. Surprisingly, calculated diffusion coefficients inside the bilayer are dependent on solute size to a lesser extent than in water and the size dependence shown by permeability is instead to be ascribed to the solute partitioning. Continuing those studies, the permeation of three real drugs across the DPPC bilayer has also been simulated [5]. The drugs are alprenolol, atenolol and pindolol, belonging to the class of β-adrenoreceptors antagonists. The simulations perfectly reproduce the experimental ranking of the permeability coefficients, and free energy calculations show that partition coefficients between water and 1-octanol overestimate the drug ability to dissolve into the membrane.

The advantage of MD simulations over conventional experiments is that the contributions from the different regions of the lipid bilayer, that is free energy, diffusion and local resistance as a function of depth, can be studied at a molecular level, whereas experimental models can only approximate the membrane as a uniform barrier slab. Further analyses of the simulations mentioned above are presented here. While the previous articles [3–5] focused on the calculation of the relevant physical properties, the aim of this paper is to investigate the behaviour of the drugs and the small organic compounds inside the membrane with atomistic detail. Therefore, flexibility, mean orientation, reorientational correlation times and hydrogen bonds will be described and, where possible, related to the observed partition and diffusion coefficients.

2. Materials and methods

2.1. Simulation protocol

The protocol of the simulations is described in detail elsewhere [3–5]. Briefly, the simulation box contained 72 DPPC molecules arranged in a 2×36 bilayer, together with 2094 water molecules (full hydration). Lipids and water were modelled using version 27 of the CHARMM force field for lipids [6]. An equilibrated starting structure of the lipid bilayer was kindly obtained from A. D. MacKerell and S. E. Feller, who participated in developing the force field. The simulation protocol was the same as that used in some of the latest Feller's simulations [6,7]. The LJ potential was switched smoothly to zero over the region from 10 and 12 Å. Electrostatic interactions were calculated via the Particle Mesh Ewald (PME) method using a κ value of 0.23 and a fast-Fourier grid density of $\sim 1 \text{Å}^{-1}$. The real space part of the PME summation was truncated at 12 Å. The SHAKE algorithm [8] was used to constrain all covalent bonds involving hydrogens. The leap-frog algorithm [9] was employed to solve the equation of motion with a time step of 2 fs. A neighbour list, used for calculating the LJ potential and the real space portion of the PME, was truncated at 14 Å and updated every 50 fs. Coordinates were saved every ps for subsequent analysis. Three-dimensional periodic boundary conditions were applied. Only the cell length normal to the membrane (L_z) was allowed to vary during the simulation to maintain a constant normal pressure (P_N) of 1 atm. The other cell dimensions (L_x and L_y) were kept fixed to maintain a constant surface area per lipid (A) of 62.9 Å^2. The pressure was maintained by the Langevin Piston algorithm [10] with a mass of 500 amu and a collision frequency of 5 ps^{-1}. The temperature (T) was maintained at 50 °C, well above the phase transition temperature of DPPC bilayers, by means of the Hoover thermostat [11]. A value of 1000 kcal ps^{-1} was used for the thermostat (fictitious) mass. The ensemble was therefore NP_NAT. The reliability of this ensemble in the context of these permeation calculations has been discussed elsewhere [3,4].

Small solutes and drugs were free to move on the x–y plane, but constrained at chosen distances from the bilayer centre (z depths) using the so-called z-constraint algorithm [3–5,12–14]. This allowed for the calculation of the force acting on the centre of mass of the permeants at different depths in the lipid bilayer. From that, the free energy difference between the water phase (outside the membrane) and those depths was directly accessible, and from the force instantaneous fluctuations, the local diffusion coefficients at those depths could be calculated. Eventually, the permeability coefficients of the solutes and drug molecules across the DPPC bilayer was obtained and their relative values found to agree favourably with available experimental data. The methods employed to insert solutes and drugs inside the DPPC membrane and to generate starting structures were described in the previous papers [3–5]. Those aspects of the methodology that are relevant to the results reported here will be briefly described. Different solutes and drugs were studied in separate simulations, but a few membrane depths were sampled in the same simulation to reduce the computational expenses while ensuring no solute–solute or drug–drug interaction occurred. For the large drugs, different orientations with respect to the membrane and different internal conformations of dihedral angles were also sampled. The β-blockers under study have six dihedral angles which were expected to be difficult to sample adequately. They, together with the structures of the drugs, are depicted in Fig. 1.

Therefore, representative drug conformations were carefully chosen and used as starting structures in separate simulations. Monte Carlo simulations in implicit solvents

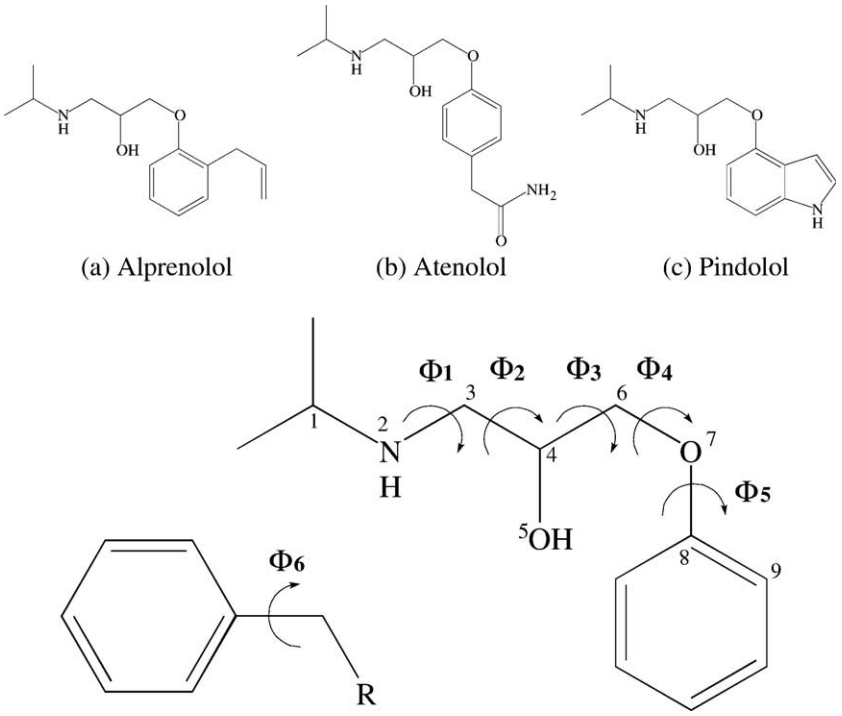

Fig. 1. Drug molecules (top) and their critical dihedral torsions (bottom). $\Phi 1 = 1-2-3-4$, $\Phi 2 = 2-3-4-5$, $\Phi 3 = 5-4-6-7$, $\Phi 4 = 4-6-7-8$, $\Phi 5 = 6-7-8-9$.

were used to determine the most populated conformations [5]. These conformers are reported in Table 1, with names for dihedral angles as in Fig. 1.

The β-blockers are elongated molecules and it was not expected that full rotation would be observed inside the DPPC bilayer. Therefore, each combination of drug conformer and membrane depth was sampled twice: once with the drug having the aromatic ring initially oriented towards the middle of the bilayer and the isopropylamine fragment towards the water phase, and once with the aromatic ring initially oriented towards the membrane exterior and the isopropylamine fragment towards the interior. However, the drugs were free to rotate during the simulations. If we name the aromatic ring as the *drug head* and the main chain as the *drug tail*, it is convenient to refer as *up* the orientation where the drug head is towards the membrane exterior and *down* the orientation where the drug head is towards the centre of the bilayer.[1]

All the simulations were run in parallel with 4 processors, using version 27 of the CHARMM software package [15], which was modified to introduce the *z*-constraint described above. The simulations were run on different Linux PC clusters with either 1 GHz Pentium III, 1.5 GHz Pentium IV, or 1.4 GHz AMD Athlon.

Table 1
The most populated combinations of dihedral angles

Drug	Φ1	Φ2	Φ3	Φ4	Φ5	Φ6
Alprenolol	292.5	82.5	180.0	300.0	127.0	202.5
Atenolol	292.5	82.5	180.0	300.0	127.0	202.5
	292.5	82.5	180.0	300.0	127.0	23.5
	292.5	82.5	180.0	300.0	307.5	202.5
	292.5	82.5	180.0	300.0	307.5	23.5
	292.5	300.0	180.0	300.0	127.0	202.5
	292.5	300.0	180.0	300.0	127.0	23.5
	292.5	300.0	180.0	300.0	307.5	202.5
	292.5	300.0	180.0	300.0	307.5	23.5
Pindolol[a]	300.0	292.5	180.0	285.0	292.5	
	82.5	292.5	180.0	285.0	292.5	
	82.5	292.5	180.0	180.0	240.0	

[a] For pindolol, the side chain is a rigid ring and there is no Φ6.

3. Results and discussion

3.1. Four region model

Since the membrane has a very inhomogeneous character when moving from one side to the other, each individual

[1] We are aware that the nomenclature usually applied is drug scaffold and drug side chain, but in the context of these simulations the use of drug head and tail is preferred. There are several reasons. Such terms recall those commonly employed for the surrounding lipids and this is useful when it comes to investigate drug–lipid interactions. Given the shape of the three β-blockers , the head and tail definitions are straightforward to understand and visualise. The name side chain here would create misunderstanding because of the presence of the second shorter chain on the aromatic ring of the drugs. Since the part of the drug molecule which is in common between β-blockers in general comprises the (3-(N-isopropyl)amino-2-idroxy)-propyl chain together with the aromatic ring, the term scaffold would not be as effective for defining the two fragments separately as head and tail. We therefore ask the reader to accept our more physical nomenclature.

leaflet has been split into four regions as described in previous publications [13,14]:

Region 1: low headgroup density, 20 to 27 Å from the bilayer centre.
Region 2: high headgroup density, 13 to 20 Å from the bilayer centre.
Region 3: high tail density, 6 to 13 Å from the bilayer centre.
Region 4: low tail density, 0 to 6 Å from the bilayer centre.

The same distinction between membrane regions has been adopted here in the interpretation of the permeation results. In what follows, unless indicated otherwise, the x-axis of all plots are along the bilayer normal, i.e., they report the z depths at which the molecules were constrained. The four regions into which each leaflet can be divided are also separated by vertical lines. Each lipid monolayer thickness is about 27 Å and further from the bilayer centre there is bulk water. A snapshot of the lipid bilayer from these simulations is reported in Fig. 2 together with a plot showing the lipid atom density distribution along the bilayer normal.

Comparisons between simulations of pure DPPC bilayers and simulations of DPPC/permeant systems (data not shown) indicate that the order parameters of C−H bonds along the lipid chains are not affected by the presence of

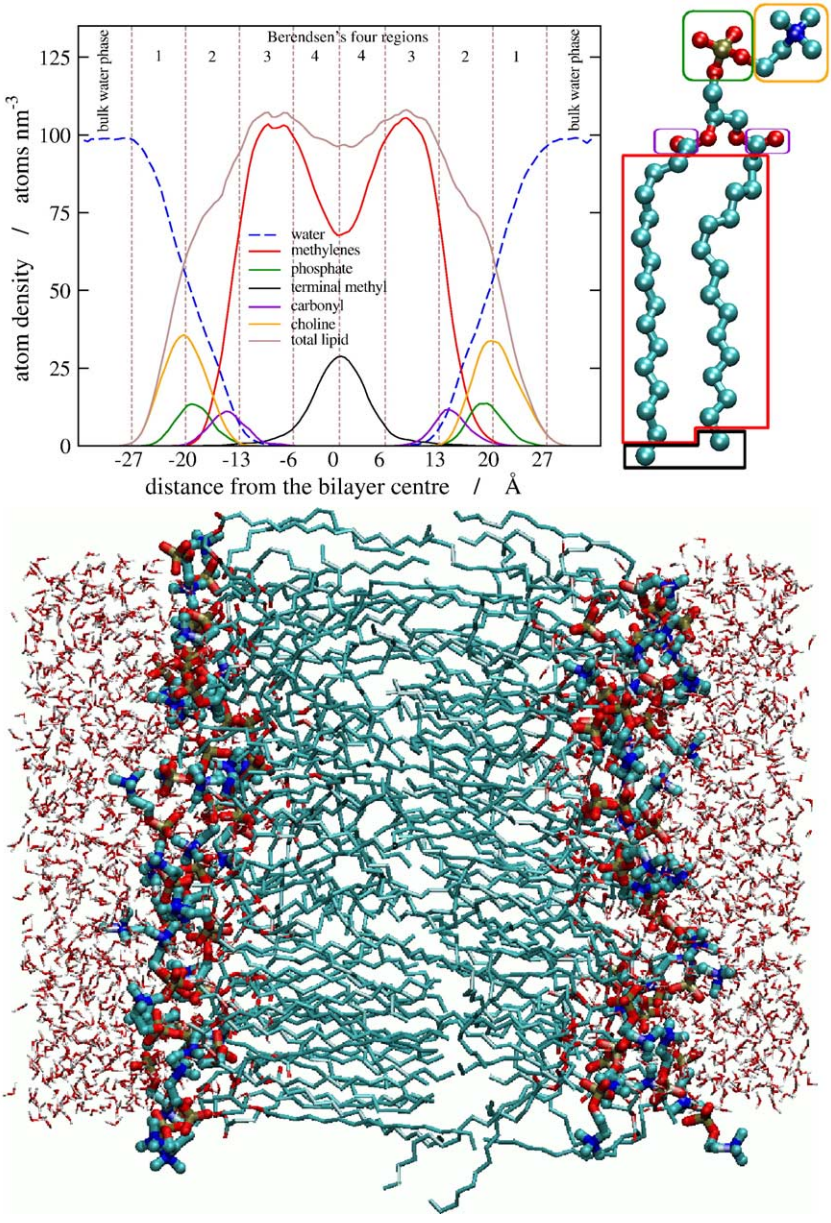

Fig. 2. Top: atom density profile. Bottom: snapshot of bilayer; blue are nitrogen atoms, red oxygen atoms, orange phosphorus atoms, cyan carbon atoms; hydrogens are omitted.

solutes or drugs. No differences in order parameter were found by Klein et al. in a simulation of 4 halothane molecules in a bilayer of 64 DPPC molecules [16]. Experiments reveal a decrease in order parameter only at high solute concentration [17]. Also, the peak-to-peak distance of the electron density along the bilayer normal with and without permeant molecules from simulations performed in our laboratory are well within the experimental range for pure DPPC bilayers [7]. Similar results were found by Stouch et al. when simulating a drug analogue in a bilayer of 36 DMPC molecules [18]. Therefore, it can be concluded that the bilayer structure is not disrupted after insertion of the β-blockers or the small organic compounds. After administration, these drugs are unlikely to saturate cell membranes. Even if this were to happen, however, related simulations of high concentrations of pentachlorophenol in a membrane suggest that the effect on the order parameters would be small [41]. Therefore, the situation modelled in this study can be thought of as representative of the in vivo conditions.

3.2. Solute flexibility

The small organic solutes are rigid molecules. Among the internal degrees of freedom, only the three drugs show interesting results.

3.2.1. Population of dihedral torsions

Owing to the density of the lipid bilayer environment, it was thought that drug dihedral torsions may not rotate significantly during the simulations. This is why the most representative dihedral conformations were selected and simulated separately. At the end of the drug/membrane simulations, it is interesting to examine the history of these torsions. It is likely that the simulations were not long enough to converge the equilibrium distribution of these angles, but some conclusions can be drawn.

The implicit solvent studies described earlier yielded slightly different results among the three drugs regarding the most populated conformers along the drug tail, which is present in all the molecules [5]. In contrast, the drug/bilayer simulations yielded identical dihedral populations for all the drugs. The populations of dihedral torsions $\Phi 1$, $\Phi 3$, $\Phi 4$ and $\Phi 5$ along the drug tail are remarkably similar among the three drugs and the different z depths. The populations of these dihedrals are shown in Fig. 3 after averaging over the three drugs and the six z depths. For clarity, the standard errors on the averages are also presented.

Different conformers for each dihedral angle were used as starting structure for separate simulations, but in the end all conformers yielded the same population distribution in all the independent simulations. Fig. 3 also shows that each dihedral torsion essentially prefers one angle only. This suggests that implicit solvent simulations are not sufficiently accurate to describe the angle distribution of these dihedrals. Only the prediction of $\Phi 3$ was accurate (i.e. 180°). For each of torsions $\Phi 1$, $\Phi 4$ and $\Phi 5$ more than one value was predicted, and these values were different from the most populated in the lipid bilayer (i.e. 180°).

Alprenolol and atenolol also have a side chain, whose first torsion, here called $\Phi 6$, yielded similar results to those in the main chain: the same distribution is found in both drugs and at all depths. However, in contrast to the dihedral torsions along the drug tail, $\Phi 6$ has two major conformations, one at around 30° and one at around 210°, the former

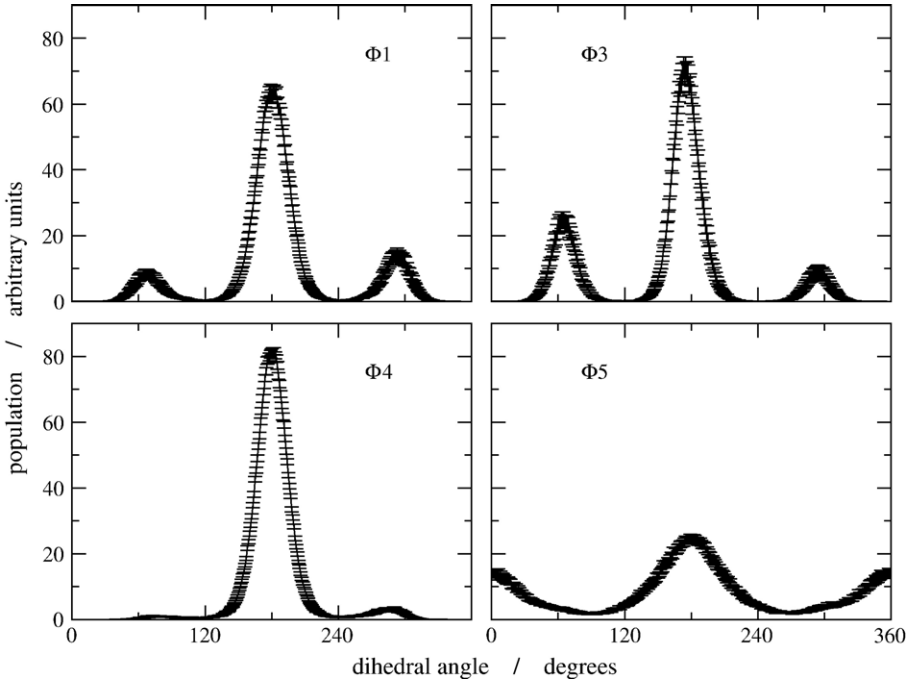

Fig. 3. Population of drug tail dihedral torsions $\Phi 1$, $\Phi 3$, $\Phi 4$ and $\Phi 5$.

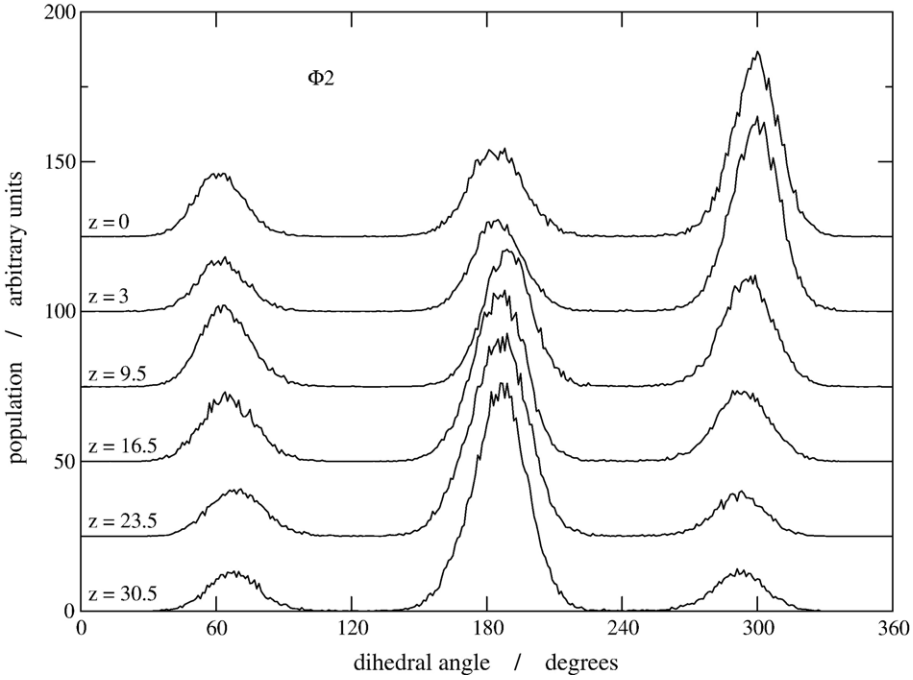

Fig. 4. Population of drug tail torsion $\Phi 2$.

with a broader distribution. In this case, therefore, the implicit solvent simulations of atenolol yielded correct results for both the values of the angle and the number of preferred conformations.

Along the drug tail, $\Phi 2$ has a unique behaviour in the drug/bilayer simulations. This torsion has a similar population for all three drugs, but adopts two different conformations at different z depths. This is shown in Fig. 4. Again, the populations reported in the figure are derived from averaging the results from the three drugs, since no significant differences exist between them. The standard errors are similar to those reported in Fig. 3.

It is clear that moving from the water phase towards the bilayer centre, values of around 180° become less and less populated, while values around 300° are more and more preferred. For this torsion, implicit solvent simulation could only find populations at 80° and 300°.

Combining the above information about the dihedral torsions, the two main drug conformations are drawn in Fig. 5: one preferred closer to the water/lipid interface, and one preferred closer to the bilayer centre.

It is clear that moving from the water phase to the bilayer centre these drugs become more elongated. This also has important consequences for the internal hydrogen bonds along the drug tail, as will be described later. Another important conclusion is that there was no real need to locate important conformers using implicit solvent and to simulate all of them in the lipid bilayer, since all yielded the same angle distributions in the end. Only one conformer needed to be simulated at each z-depth in the up and down orientation for each drug, reducing considerably the number of simulations required. This could not have been determined a priori, but this conclusion makes future work easier and computationally less demanding.

Simple conformational analysis of the three drugs simulated here was performed by Palm et al. in vacuum [19] and in chloroform and water, using a continuum representation of the solvent [20]. Details concerning some of the dihedrals are reported for the calculations in vacuum only. Only the value of torsion $\Phi 4$, which is mostly around 180°, agrees in both Palm's publication and in this lipid bilayer. Results for $\Phi 2$ and $\Phi 3$ disagree. The difference in the value of $\Phi 2$ also has consequences for the intramolecular H-bonds, as will be explained later.

3.3. Hydrogen bonds

The hydrogen bonding ability of the drug molecules is important because it is often correlated with drug partitioning in organic solvents and drug permeability. The following criteria were adopted for the identification of an H-bond [21]: the distance between the donor and the acceptor atoms (oxygen or nitrogen) is less than or equal to 3.25 Å and the angle between the vector linking acceptor and donor atoms and the donor–hydrogen bond is less than or equal to 35°. For the three β-blockers , both external (intermolecular) and internal (intramolecular) H-bonds occur. For the small organic compounds, only external H-bonds are possible.

3.3.1. H-bonds for the small solutes

The number of H-bonds between the permeants and the surrounding waters and lipids is plotted in Figs. 6 and 7 as a function of depth. The number of H-bonds involving a molecule is counted during the simulation and then

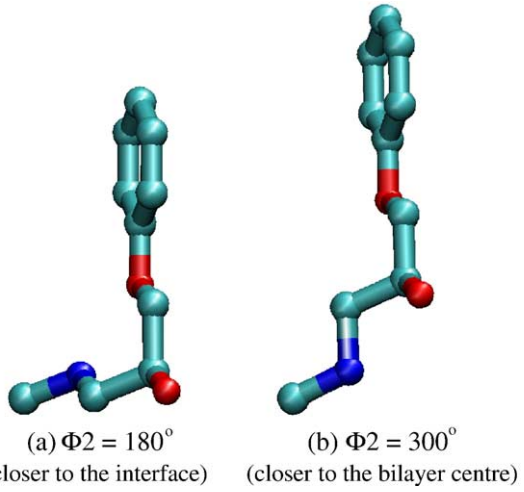

Fig. 5. The two major drug configurations. Drug side chains, hydrogens and the two $-CH_3$ groups forming the isopropyl fragment at the end of the drug tail are not shown for clarity.

divided by the number of coordinate sets analysed. The numbers plotted in Figs. 6 and 7 are thus the mean numbers of H-bonds per simulation frame, or in other words the mean instantaneous number of H-bonds. These are also averaged over the five identical solutes which are constrained at the same z depth in separate simulations and, from the differences between them, the standard errors are obtained.

Despite the strong polarization of the O−H bond, which is modelled in atomistic simulation with a charge of −0.834 e on the oxygen and +0.417 e on the hydrogen, water is not always the solute involved in the largest number of H-bonds. Nitrogen-containing solutes, namely acetamide and methylamine, generally form more H-bonds than oxygen-containing solutes, namely acetic-acid and methanol, although the differences are very small.

It should be noted that H-bonds between polar permeants and water are non-zero even in the hydrocarbon core of the membrane (regions 3 and 4), although their number is much lower than closer to the interface (regions 1 and 2). The hydration in the middle of the bilayer was analysed in further details for one of the simulations involving acetic acid, since that gave an extremely long-lived H-bond with water at the bilayer centre ($z=0$). At the end of the simulation, a column of water molecules enters the membrane and reaches the acetic acid molecule as depicted in Fig. 8.

The acetic acid orients its polar fragment towards the water/lipid interface and towards the water column. A hydrogen bond network is clear: oxygen and hydrogen atoms alternate in the column. After studying the "history" of the water column, it was found that a single water molecule entered the hydrocarbon core, reaching the acetic acid in the middle of the membrane and H-bonding to it. This occurred 0.55 ns after the beginning of the simulation. This "complex" was very stable and lasted for about 1 ns. For 0.6 ns, the complex freely rotated around the solute centre of mass and moved on the x–y plane, then other water molecules began moving towards the water/acetic acid complex, which at that moment was oriented with the water towards the headgroup region. After 1.3 ns from the beginning of the simulation, a first column of water was formed, similar to that of Fig. 8. After this, the complex stopped rotating and reduced its motion in the x–y plane. After another 0.2 ns, this first column was disrupted and only two water molecules remained hydrogen-bonded to the

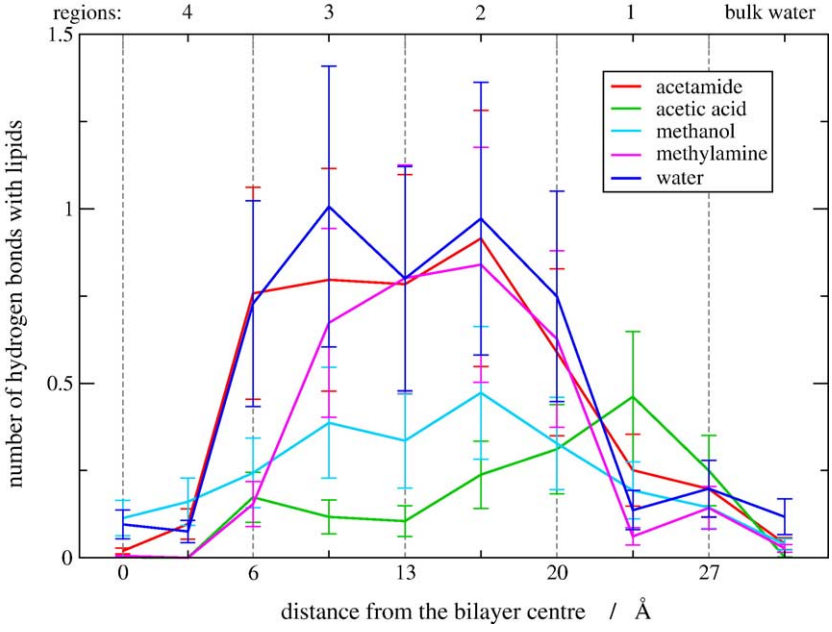

Fig. 6. Hydrogen bonds between small organic solutes and surrounding lipids.

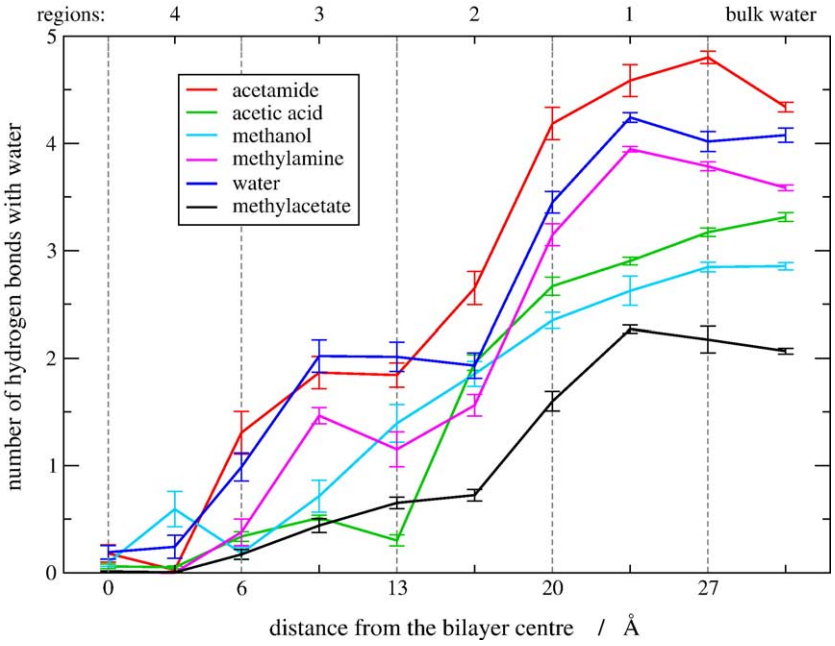

Fig. 7. Hydrogen bonds between small organic solutes and surrounding water.

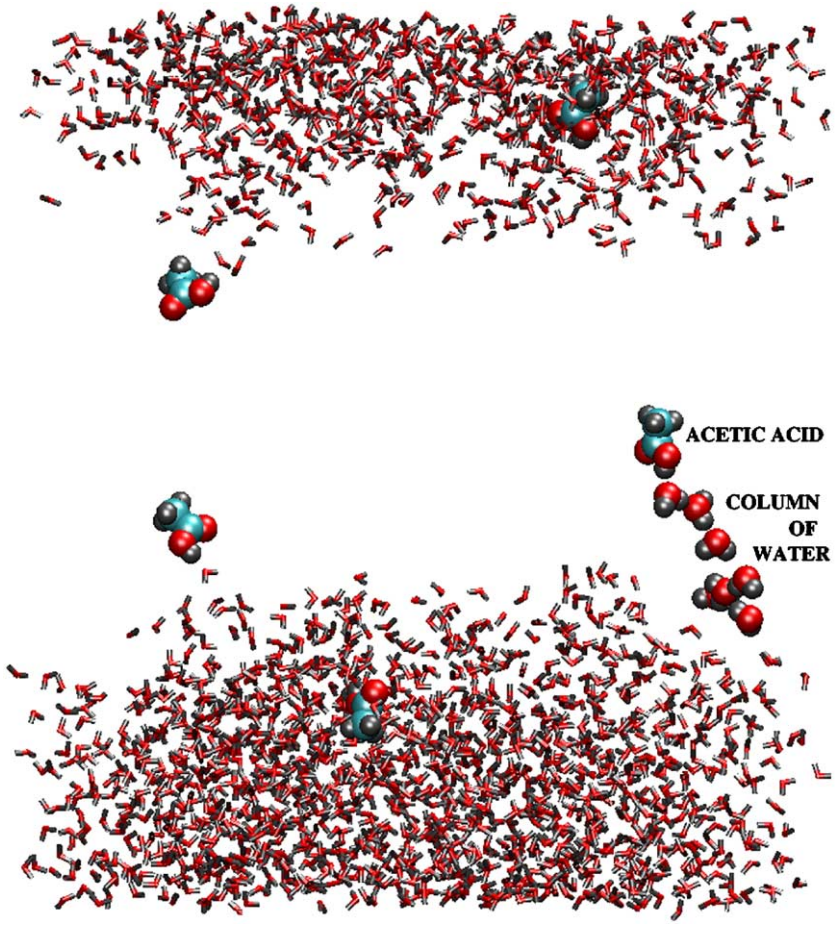

Fig. 8. Hydration of acetic acid. The water layers on the two sides of the membrane are shown. For clarity, lipids are omitted. Acetic acid and water molecules forming a column hydrating the solute are highlighted.

acetic acid in the middle of the bilayer, including the first which reached the solute 0.9 ns earlier: one molecule hydrated the carbonyl oxygen of the acetic acid and the other hydrated the hydroxyl group. This new three-membered di-hydrated complex was again free to rotate around the centre of mass of the acetic acid and to move in the x–y plane. After another 0.2 ns, a second column of water was formed, but this time with water molecules belonging to the opposite side of the bilayer. This column of water was still present at the end of the simulation. However, the individual water molecules in the column exchanged their relative positions, some left and new water molecules arrived. The closer the water to the acetic acid, the longer it stayed in the column. The first water reaching the solute remained complexed for about 1 ns, until 1.55 ns after the simulation started. Eventually, it swapped its location with the second water in the column twice in the space of 0.1 ns, and then finally left. Remarkably, it moved towards the opposite side of the bilayer to that from which it entered. Therefore, in less than 2 ns, this water molecule crossed the entire thickness of the lipid membrane. The history of the column of water molecules is shown in Fig. 9.

Similar water fingers entering the membrane and hydrating permeating solutes were also found by other workers in a simulation of valproic acid in a DPPC bilayer [22]. These observations suggest that acetic acid may in fact permeate biological membranes as a dimer either with water or with another acetic acid molecule. Such behaviour may also be a common feature of all highly hydrophilic compounds and may facilitate the permeation process. We would like to stress that the water molecules were not dragged during the simulation, they spontaneously found their way into the membrane core. Nor was acetic acid pulled from a location in water to the location at the bilayer centre carrying its hydration shell with it (like in the valproic acid study by other workers [22]), but rather the starting structure was generated separately with the solute completely surrounded only by the lipid hydrocarbon chains. Water thus diffused to hydrate the solute from the water phase.

From these simulations, we cannot say in a definitive way how such water columns would behave when other biologically relevant molecules like amino acids or sugars are permeating, or whether the latter molecules would be able to replace the water in their interaction with drugs during membrane permeation. In this study, the possibility for solutes to permeate as small oligomers or to permeate together with their hydration shell is not addressed and remains unresolved, although the observations regarding the column of water do not rule out such mechanisms.

3.3.2. Drug external H-bonds

The mean number of H-bonds per simulation step between the drugs and water molecules is plotted as a function of depth in the lipid bilayer at the top of Fig. 10.

For each drug, the total number of H-bonds is plotted with a solid lines. The contribution of each functional group is represented as a fraction of the total number and plotted with a dashed line. The distance between adjacent lines represents the number of H-bonds formed by the specified group.

Although the number of H-bonds is very small in region 4, hydration occurs at all depths, showing that some water penetration of the bilayer core is taking place. This is

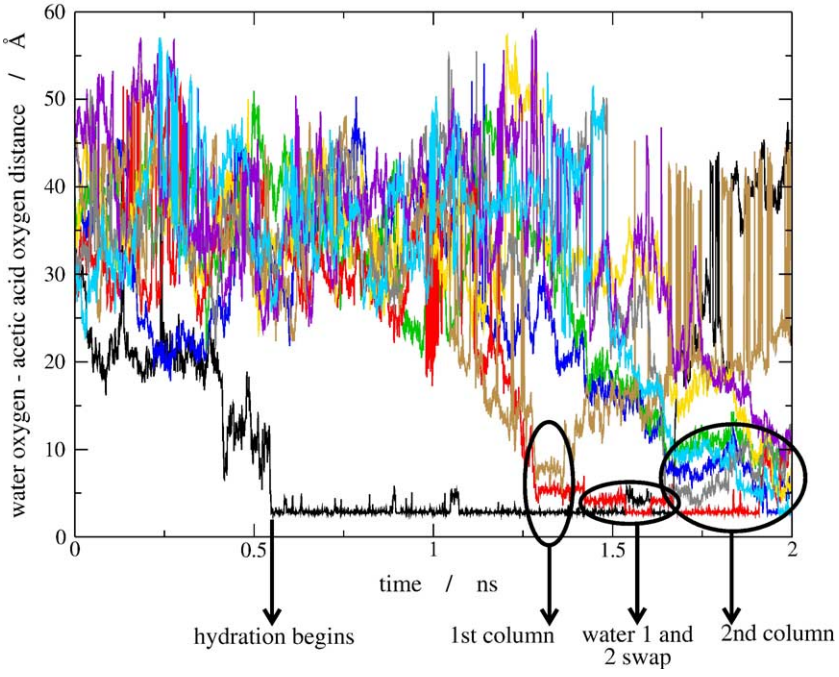

Fig. 9. History of the water molecules hydrating the acetic acid constrained in the middle of the bilayer.

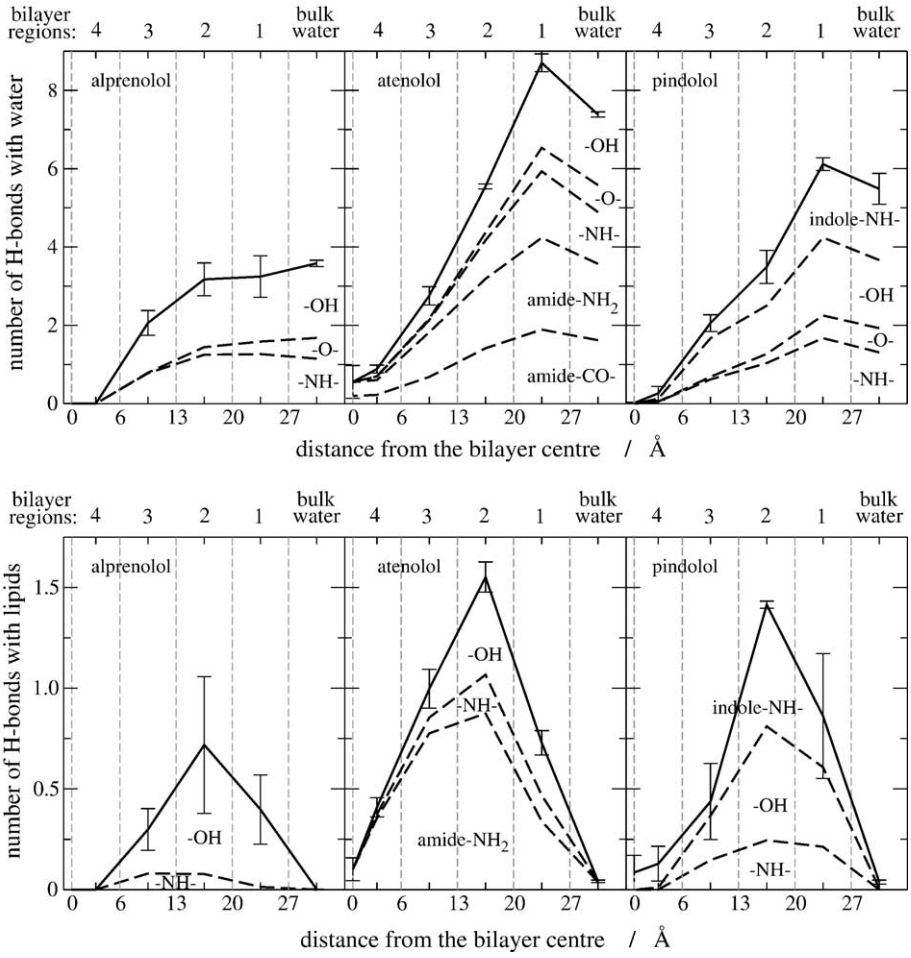

Fig. 10. Top: mean number of H-bonds between drugs and water molecules. Bottom: mean number of H-bonds between drugs and surrounding lipids. Functional groups: –OH, –NH– and –O– are the hydroxyl, the secondary amine and the ether group respectively along the drug tail; amide and indole groups are on the side chains.

consistent with the results for the small organic compounds reported in the previous section. The number of H-bonds with water involving the drug tail groups is remarkably very similar among the three drugs and therefore well represented by the number of H-bonds made by alprenolol, since this drug does not have any hydrogen bonding groups on its side chain. As expected, most of the H-bonds on the drug tail involve the –OH and –NH– groups, while the ether oxygen forms very few. Moving from the water phase towards the middle of the lipid bilayer, all the drug tail functional groups decrease the number of H-bonds with water uniformly. Regarding the side chains, the indole –NH– group in pindolol is involved in about as many H-bonds as the –NH– group in the drug tail. In total, pindolol forms about 1.5 times the number of H-bonds of alprenolol. The amide –CO– and $–NH_2$ groups together in atenolol form about as many H-bonds as the three groups in the drug tail, and in total atenolol forms approximately double the H-bonds of alprenolol.

The bottom of Fig. 10 reports the number of H-bonds between drugs and lipids. Since lipids do not have hydrogen bonding donors, the ether oxygen on the drug tail and the amide carbonyl oxygen on atenolol's side chain cannot be involved in H-bonds with the surrounding lipids. As with water, the amide group in atenolol forms most of the H-bonds. For the drug tail, in contrast to what happens with water, –OH forms many more H-bonds than –NH–.

It can be noted that the number of H-bonds between water and these drugs roughly reproduces the ranking of free energies and permeabilities of the three β-blockers [5]. This helps to understand why the H-bonding possibilities are an important parameter in common QSAR methods which try to predict the fraction of drug absorbed after oral administration, or the fraction of drug penetration across the blood/brain barrier. For the three drugs under study, a trivial model which simply counts the number of H-bonds could have given the same permeability ranking as the extensive simulations and free energy calculations. However, these simulations do offer significant advantages. First, this trivial hydrogen bonding model works for the three β-blockers simulated here but it cannot be guaranteed that it would work for every drug. Simulations similar to those performed here can hopefully predict the cases where the trivial H-bond model will not work. Second, the hydrogen bonding possibilities are best evaluated by means of MD simulations,

which take into account the molecular flexibility and dynamics, rather than by means of static structures generated from standard chemical geometries. Third, simulations can possibly work in those situations where the count of H-bonds is found not to correlate directly with the permeability ranking, for example, when studying drug entities which belong to different families and have different functional groups. Simulations can also help to understand those cases where the simple count of H-bonds does not work, since simulations yield atomistic details which are not accessible from experiments.

3.3.3. Drug internal H-bonds

Owing to the flexibility of the drug molecules, internal H-bonds between pairs of functional groups can be formed. No H-bonds could be counted between the side chain groups (amide in atenolol and indole in pindolol) and any of the drug tail groups. In the drug tail, no H-bonds were found between the ether oxygen and the hydroxyl group. In contrast, some H-bonds involving amine-ether and amine-hydroxyl pairs were observed. These are shown in Fig. 11, averaged over all the simulations, at different z depths in the lipid bilayer. The total number of intramolecular H-bonds is plotted with a solid line, and a dashed line separates the contributions from the two pairs.

The number of intramolecular H-bonds varies at different depths, but considering the error bars, one could argue that it stays quite constant moving from region 1 to region 4. Looking at the contributions, the number of H-bonds involving –NH– and ether oxygen decreases significantly going deeper into the membrane interior, while the number of H-bonds involving –NH– and–OH increases by a similar amount. The sum of the two effects is that the total number of intramolecular H-bonds does not change significantly in different membrane regions. Therefore, from these simulations, the loss of H-bonds between the drug and the surrounding lipids or waters when moving from the water phase towards the middle of the membrane is not compensated by an increase in the number of intramolecular H-bonds.

The preference for the –NH– group to form intramolecular H-bonds with the ether oxygen when closer to the interface and with the–OH group when closer to the bilayer centre is related to the drug conformation, as mentioned earlier. Closer to the interface the drug is more folded on itself, the amine and ether groups point on the same side of the molecule while the hydroxyl faces the opposite side. Closer to the bilayer centre the drug is more elongated and the amine group points on the same side as the hydroxyl. Thus, the coformations reported in Fig. 5 effectively determine which intramolecular hydrogen bonds can form. Assuming that the overall drug conformation is more folded or more elongated because of steric constraints due to lipid packing, the possibility of maintaining a fairly constant number of intramolecular H-bonds by varying the pair of functional groups involved may facilitate the overall conformational change.

Difficult to explain is the overall higher number of intramolecular H-bonds for alprenolol (first plot on the left hand side in Fig. 11). Considering the error bars, the difference with respect to the other two blockers may be not significant. However, this seems to be a general trend in all regions but 4 (the membrane centre). This difference does not affect visibly the amount of H-bonds with lipids and waters because the latter are in much larger number, so arguably it does not make a significant contribution to the overall permeation mechanism. Although the higher propensity for alprenolol to form intramolecular H-bonds remains unresolved, it is interesting to note (see subsequent sections) that the orientational behaviour of alprenolol in the membrane also differs from that of the other blockers. It should also be noted that only atomistic simulations would be able to resolve these subtle effects.

3.4. Orientation

The orientation with respect to the lipid membrane was studied for the three drugs and for the largest among the small organic compounds: benzene, methylacetate, acetic

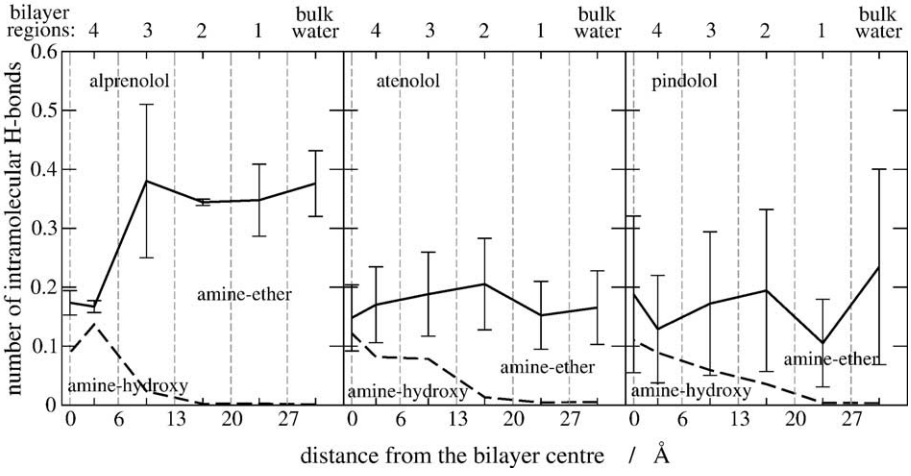

Fig. 11. Mean number of intramolecular H-bonds between pairs of functional groups.

acid, acetamide. For the latter, the orientation is for the main plane of the molecules: the aromatic ring in benzene, the plane of the four atoms bound to the carbonyl carbon in methylacetate, acetic acid and acetamide. For the drugs, the orientation of the aromatic ring and that of the overall molecule are studied separately. In some of the small organic solutes, a polar group is easily identifiable and it is possible to construct a vector connecting that group with the apolar fragment. The orientation of such a vector is investigated for methanol, methylamine, acetic acid and acetamide. For the β-blockers instead, this is not done, as polar and apolar groups alternate on both the main and side chains. For the drugs, therefore, the analysis of such groups is implicitly included in the hydrogen bond analysis.

3.4.1. Overall orientation of small solutes

A measure of the degree of order in a particular system is given by the order parameter S:

$$S = \frac{1}{2}\langle 3\cos^2\theta - 1\rangle \quad (1)$$

Here, θ is the angle between the normal to the principal plane of each solute and the normal to the lipid bilayer, the brackets denote an ensemble average. S varies between 1.0 (indicating full order perpendicular to the bilayer normal) and −0.5 (indicating full order along the bilayer normal). A value of zero is considered to indicate that full isotropic motion is occurring. Fig. 12 plots the solute order parameter as a function of depth in the bilayer. Standard errors are calculated from the difference of the mean $\langle S\rangle$ in each of the individual simulations from their overall average value for each depth.

It can be seen that moving from the water phase towards the membrane interior, the permeants tend to be aligned parallel to the lipid tails. This was expected, since the lipid molecules are tightly packed because of interfacial constraints, and the free space for solute permeation is therefore parallel to the bilayer normal. For all the compounds, the greatest disorder, i.e., S closest to 0, occurs in bulk water and in region 1, as expected. The highest order parallel to the lipid tails, i.e., S closest to −0.5, occurs in region 3. In region 4, in the lower part of the lipid chains, the solutes are preferentially ordered along the bilayer normal but to a lesser extent than in the upper part of the chains, primarily because of the lower density and the higher lipid mobility in region 4. The value of S is closest to −0.5 for benzene, which is the largest compound among those studied. However, the difference in order parameter among the solutes is very small and arguably the size is not the most important factor determining the solute orientation.

Interestingly, at 27 Å far from the bilayer centre, i.e., at the interface between bilayer and bulk water phase, the benzene molecule tends to lie on the lipid heads parallel to the bilayer surface, and this may be related to the behaviour of the phosphorus–nitrogen vector in the choline fragment, which tends to lie on the bilayer plane. Remarkably, the same behaviour was found in simulation studies of indole molecules inside a POPC bilayer [23]: the order parameter of these aromatic molecules is reported to be positive in the headgroup region and negative in the membrane interior, with values in region 4 closer to 0 than those in region 3.

Results from these simulations therefore suggest that the solutes have a preferred orientation, to a greater or lesser extent. This is in contrast to that reported in previous simulations of benzene molecules inside a DMPC bilayers [17,24,25]. However, the surface area per lipid in that system was about 66 Å^2, while here it is 62.9 Å^2. When the benzene molecule is more tightly packed in the lipid environment, its orientation is preferentially parallel to the lipid chains. Moreover, the simulation temperature was the same as that employed here, but DPPC bilayers enter the biologically relevant liquid-crystalline phase at 42 °C, while DMPC enters at 22 °C [26]. When the lipid bilayer is more fluid, permeants can move and rotate to a larger extent. No direct experimental studies have been found in the literature regarding benzene or the other small solutes simulated here. However, the preferred orientation parallel to the bilayer normal was reported for long chain alkanes [27,28], fluorescent probes [29] and drug molecules [30,31].

The findings from these simulations regarding the preferred solute orientation inside the lipid bilayer agree with the experimental observation that water/membrane partitioning is highly affected by entropic effects, as mentioned in the previous paper [4]. In those analyses, the theoretical model, which uses the Barclay–Butler relationship between entropy and enthalpy of solvation, had no experimental confirmation, since the experiments do not yield atomic details. In contrast, these simulations offer such details and support the previous hypothesis: when moving from water into the membrane, solutes lose degrees of freedom, because they are forced to stay oriented parallel to the lipids. For molecules larger than those studied here, this effect is expected to be even stronger, and so it can be argued that partitioning into lipid bilayers, and in turn permeabilities, are also highly size-dependent properties. This supports the idea that, as reported in the previous article [4], the size dependence of permeability coefficients is mainly to be ascribed to size-dependent partitioning rather than diffusion. That lipid packing affects solute partitioning into membranes finally explains the significantly lower partition coefficient of benzene in the middle of the lipid bilayer than in hexadecane, as shown previously [3,4].

3.4.2. Polar group orientation in small solutes

In some of the small organic compounds, a polar vector is identified as the vector linking the carbon atom and its heteroatom(s): the C − O bond in methanol, the C − N bond in methylamine, the vector connecting the carboxyl carbon with the centre of geometry of the two carboxyl oxygens in acetic acid, the vector connecting the carbonyl carbon with the centre of geometry of oxygen and nitrogen in acetamide.

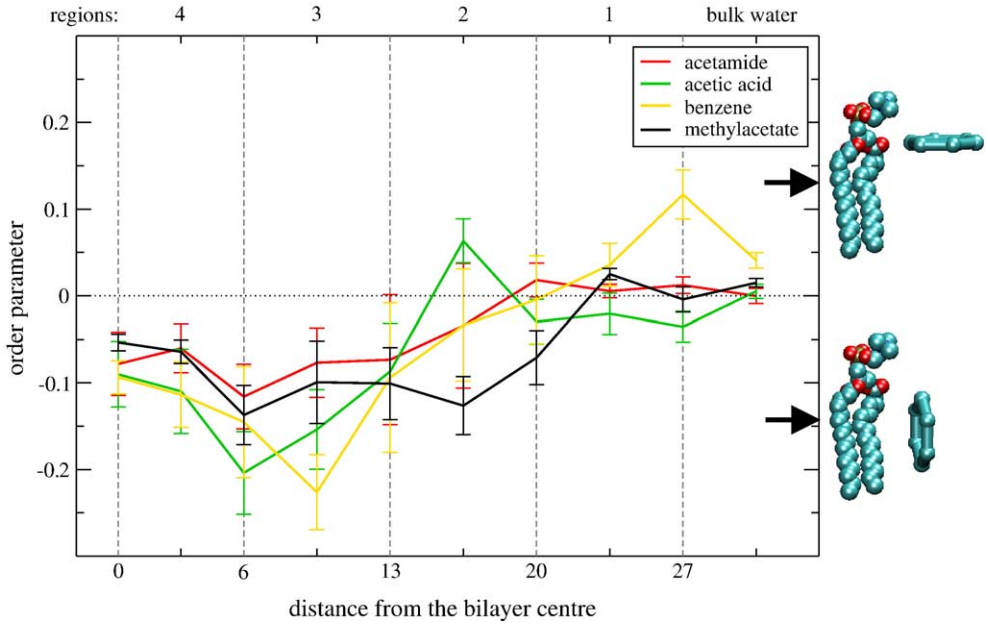

Fig. 12. Solute order parameter as a function of depth. For clarity, a picture indicates the physical meaning of positive and negative values of S. In that picture, the size ratio between lipid and solute (benzene) molecules is not respected.

The direction of the vector is from the carbon towards the heteroatoms. From the angle between the polar vector and the bilayer normal, an order parameter was calculated and plotted in Fig. 13.

In this case, a value of 1 indicates full order parallel to bilayer normal and a value of −0.5 full order perpendicular to the bilayer normal. Results agree with those plotted in Fig. 12: the polar vector is mostly oriented parallel to the lipid chains, above all in the densest regions 2 and 3. To understand whether the polar group is oriented towards the water phase or the hydrocarbon core of the membrane, the ratio between the z component of the polar vector and its total length was calculated and plotted in Fig. 14.

This yields the cosine of the angle between the polar vector and the bilayer normal, in other words the Legendre polynomial of first order. A value of 1 indicates that the polar group is oriented towards the water phase and a value of −1 indicates that the polar group is oriented towards the middle of the bilayer. A value of zero does not necessarily mean that the polar vector is oriented perpendicular to the bilayer normal, but rather that on average there are as many vectors oriented towards the water phase as towards the

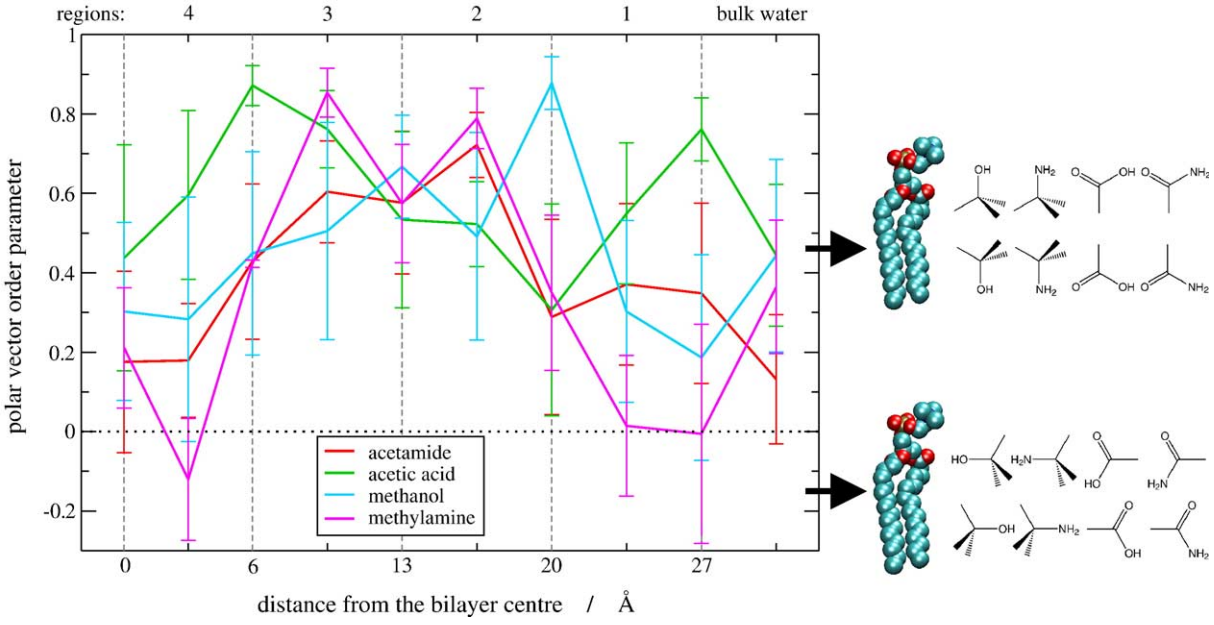

Fig. 13. Polar vector orientation with respect to the bilayer normal.

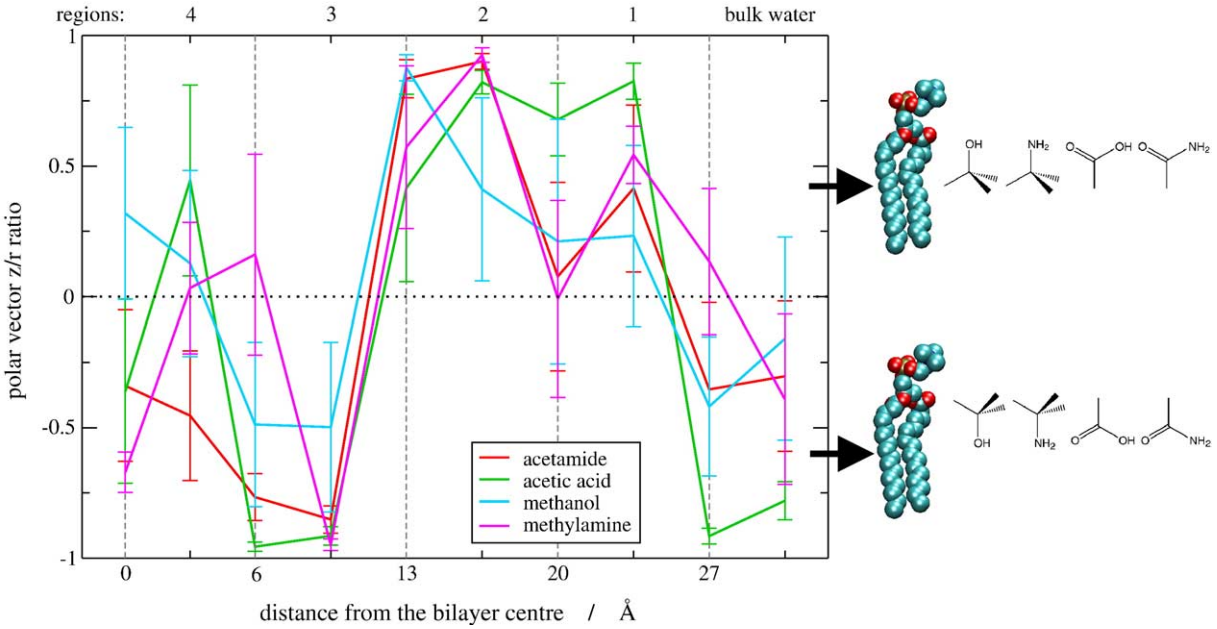

Fig. 14. Ratio between the z component of the polar vector and its total length.

membrane interior. This is the reason why neither the polar vector order parameter nor the z/length ratio are sufficient, when considered alone, to give a complete picture of the solute orientational behaviour. Interestingly, polar groups tend to be oriented towards the lipid headgroups when the solutes are closer to the interface, while they tend to be oriented towards the centre of the bilayer when the solutes are in the middle of the membrane. Lipid headgroups are highly charged and have oxygens available for H-bonds, so it is thought that short range electrostatic interactions and local hydrogen-bonding networks may be responsible for the behaviour of the permeants at the interface. Moreover, when the polar group is oriented towards bulk water, the alkyl part can penetrate the hydrocarbon core of the membrane. This kind of solute orientation is also reported for drug molecules by both experiments [30,31,32,33] and simulations [18]. On the other hand, it is hard to understand the behaviour observed at the end of region 3 where the polar groups tend to be oriented towards the centre of the membrane. It is expected that, when the solutes are in the middle of the bilayer, the interactions with the headgroups and waters are negligible and they do not affect the solute orientation. This is indeed what happens in region 4.

3.4.3. Drug head orientation

The orientation of the aromatic ring representing the drug head was studied by calculating the Legendre polynomial of rank 2 (S) for the angle between the normal to the ring plane and the bilayer normal. Its average over the simulation time and eventually over the conformers sampled is plotted in Fig. 15 as a function of z depth in the lipid bilayer.

At $z=30.5$ Å, S is zero for all the drugs. This value indicates full isotropic motion and random distribution of atoms. This value was expected because at this position, drugs are still in the water phase and can freely rotate around their centre of mass.

Deeper into the membrane S is significantly different from zero. Owing to the orientation of the lipid molecules and the tight lipid packing, negative values were expected in the membrane interior, indicating that the plane of the aromatic ring parallels the bilayer normal. In contrast, positive values were also found. For atenolol and pindolol this mainly occurs in region 2, while for alprenolol, it happens in region 3. In these cases, the plane of the drug head lies perpendicular to the bilayer normal. The reason for this behaviour seems to be the possibility for the drug to form a larger number of H-bonds, with the differences between the drugs arising from the different distribution of polar fragments on the side chains. That drug molecules prefer to stay tilted with respect to the bilayer normal in order to optimize their hydrogen bonding with their environment was observed by Stouch et al. in a simulation of a nifedipine analogue located near the interface of a DMPC bilayer [18].

The conclusion is that hydrogen bonding opportunities should be considered along with steric restraints in determining the permeant orientation. When hydrogen bonding sites can be satisfied, the solute prefers to stay parallel to the bilayer normal, because this orientation does not require modifying the bilayer's stable structure. However, when H-bonds cannot be formed, the lipid molecules can actually rearrange themselves to make their formation possible. The experimental observation that solute permeation is reduced in those conditions where the lipid packing is higher, for example, with increasing concentration of cholesterol or at lower temperatures [34–38], is explained on the basis of solute exclusion, i.e., on the basis of more

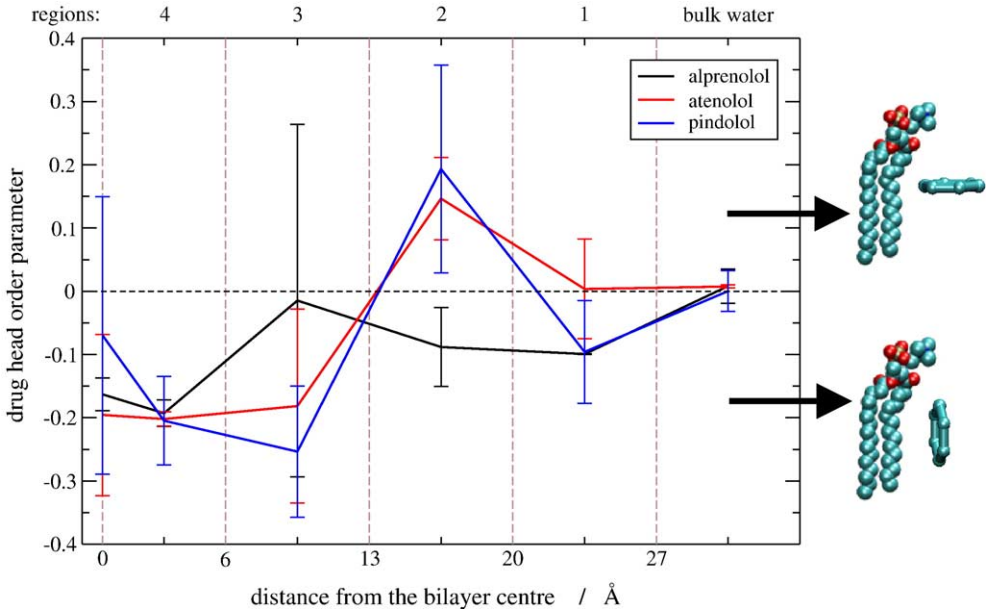

Fig. 15. Order parameter of drug head as a function of z depths.

work required to form a cavity able to host a solute. These simulations offer an additional explanation: when lipid packing is higher solutes cannot optimize their hydrogen bonding network because they cannot orient themselves to form the largest amount of H-bonds. This in turn reduces solute partitioning into the membrane and finally its permeation.

3.4.4. Drug vector: up and down orientations

The overall drug orientation is studied by investigating the vector linking the centre of geometry of the drug head and the centre of geometry of the drug tail. Its orientation is investigated by calculating the cosine of the angle between the vector and the bilayer normal. This is the Legendre polynomial of rank 1 of that angle, and is referred to in these analyses as the drug vector P_1. Obviously P_1 can range between +1 and −1. A value of zero indicates either that the drug lies perpendicular to the bilayer normal, or that it can freely interconvert its orientation up→down and down→up without any restrictions. An absolute value of 1 indicates instead that the drug is completely parallel to the bilayer normal. The sign has the following meaning: a positive value indicates the drug is in the down orientation, and a negative value indicates the drug is in the up orientation. Results from these simulations are plotted in Fig. 16, together with a picture of the drug in the up and down orientation. For each saved coordinate set (one every ps) P_1 is calculated and averaged over the full simulation length. This average is $\langle P_1 \rangle_t$, with $\langle \ldots \rangle_t$ indicating a time average. For atenolol and pindolol Fig. 16 plots the further average among the individual conformers with the associated standard errors. For alprenolol, Fig. 16 plots $\langle P_1 \rangle_t$ and the errors are calculated by dividing the single simulation into frames of 200 ps. When the drug orientation in the starting structure of the simulation was UP, the average drug orientation is plotted with a solid line. When instead the drug was in the DOWN orientation in the starting structure, the average drug orientation from the simulation is plotted with a dashed line. Therefore, the terms UP and DOWN inside the plot legend refer to the orientation in the starting structure which yielded that plot. The terms UP and DOWN on the picture of the molecules simply show that when P_1 is positive the drug orientation is DOWN and that when P_1 is negative the drug orientation is UP.

At the furthest distance from the bilayer centre (z=30.5 Å) P_1 is basically zero in all plots. At this position, drugs are still in water phase and they can freely rotate. Studying the time evolution of P_1 in the single simulations reveals that the value of zero does not derive from the drugs lying on the membrane plane, but rather the drugs have isotropic motions and can freely change their orientation, with P_1 spanning over the entire range from +1 to −1. Between 10 and 20 clear and net interconversions (up→down and down→up) could be counted for alprenolol (whose simulations lasted 4 ns), and between 5 and 10 interconversions for atenolol and pindolol (simulations lasted 3 ns).

Inside the membrane, a higher degree of order is found. Here, drug orientation is difficult to study because of the long time scale of these motions with respect to the short time scale of computer simulations. In Fig. 16, if the solid lines do not reach positive values and the dashed lines do not reach negative values, it means that the drug orientation in the starting structure (either up or down) is maintained for most of the simulation and most of the conformers. However, from Fig. 16, it appears clear that this happens in the case of atenolol only. Although the starting orientation is still preferred, even for this drug, up→down and

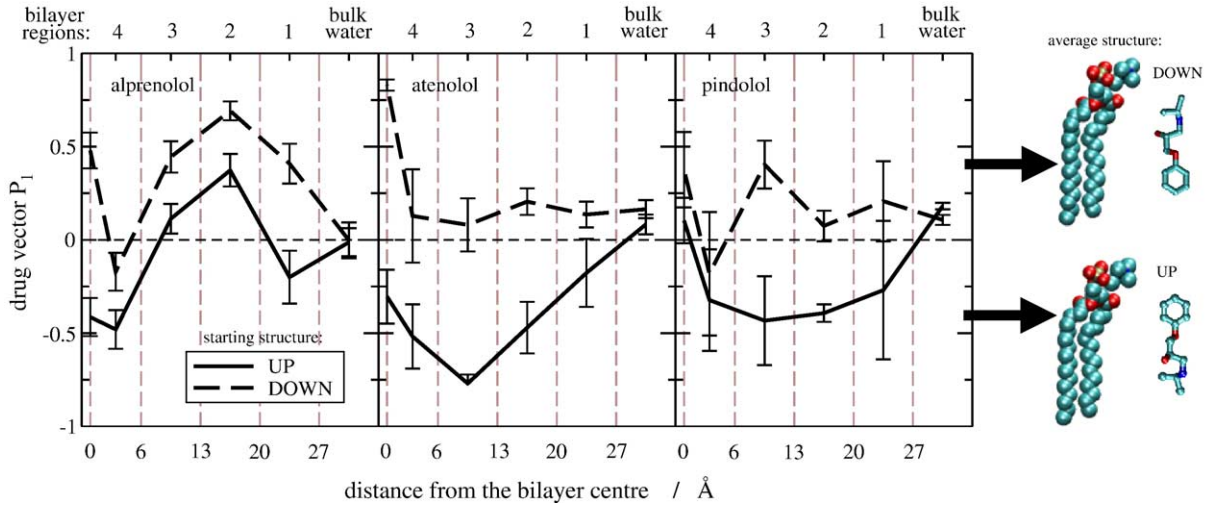

Fig. 16. Drug vector P_1 as a function of depth in the lipid bilayer. See text for definitions.

down→up interconversions occurred at all z depths. For alprenolol and pindolol, the starting structure is preferred at most of the z depths but not all of them, and up→down or down→up interconversions occurred at all depths. For alprenolol in particular, the preferred orientation was down for both starting structures in regions 2 and 3. Although solid and dashed lines cross the zero line, starting from the up or the down orientation did not yield the same profile; the two curves still differ. This suggests that the simulations were not long enough to draw any conclusion about the equilibrium distribution of orientations of these drugs inside a lipid bilayer, explaining why $\Delta G(z)$ profiles from the two orientations differ [5].

Further important information may be obtained from these analyses. Looking again at Fig. 16, it can be seen that on average for atenolol the solid line has higher absolute values than the dashed line. This suggests that for atenolol the up orientation is more conserved than the down orientation. In other words, the drug which possesses a side chain on its head with a highly polar group able to form a large number of long-lived H-bonds prefers to stay with the head up towards the water phase rather than down with the head towards the membrane interior. The inverse situation can be described for alprenolol. This drug does not have the possibility to form H-bonds with the side chain on its head, but it still has hydrogen bonding ability on its tail. Fig. 16 shows that the alprenolol down orientation, with the tail oriented towards the water and the head towards the bilayer centre, is indeed preferred, even when the starting structure contained an up orientation (in regions 2 and 3). The situation is somewhere in between for pindolol. It can form H-bonds with the side chain on its head, but not as many as the amide group on atenolol. In the end, the curves for pindolol are more similar to those for atenolol than to those for alprenolol.

These findings agree with experimental observables that predict a drug orientation inside biological membranes such that the hydrophobic parts of the molecules are placed towards the membrane interior and the hydrophilic ones towards the lipid/water interface [30–33,39]. The drug vector orientation is also in agreement with the drug head orientation described in the preceding section.

3.4.5. Drug vector: parallel or perpendicular to bilayer normal

Drug orientation is not however completely described by the value of P_1.

When several conformers are studied for the same drug at the same z depth and with the same starting orientation (up or down), as was done for atenolol and pindolol, in one simulation the molecule may stay in the same configuration as in the starting structure and then interconvert just in the very last steps, whereas in another simulation it may interconvert just a few steps after the beginning and stay in the new orientation for the rest of the simulation. The average orientation from the two simulations would then predict $\langle P_1 \rangle \approx 0$, i.e. either that the drug lies perpendicular to the bilayer normal or that it experiences isotropic motions. The first interpretation is not true, as in both simulations the individual P_1 values were close to +1 and −1 respectively. The second interpretation is not true either, as one interconversion only occurred in the simulations and one cannot conclude that the drug molecules can freely rotate. Only the error bars can give an indication that these interpretations are too simplistic.

The conclusion is that $\langle P_1 \rangle_t$ plotted in Fig. 16 can only indicate if on average the drugs are in the up or down orientation and if they maintain the orientation of the starting structure. To know whether they tend to stay preferentially parallel or perpendicular to the bilayer normal, the order parameter of the drug vector is more appropriate. The order parameter of the drug vector is here called P_2 and is calculated in the same way as for the drug head, i.e., from the Legendre polynomial of rank 2 of the angle between the drug vector and the bilayer normal. A

value of P_2 equal to 1 indicates that the drugs are aligned parallel to the bilayer normal, a value of −0.5 indicates that the drugs lay parallel to the bilayer surface. P_2 values are plotted in Fig. 17, together with a picture showing the meaning of the values.

At z=30.5 Å, all three drugs have $P_2 \approx 0$, confirming that $\langle P_1 \rangle_t = 0$ at that z depth was really due to isotropic motions. Inside the membrane, most of the values are positive, meaning that the drug molecules tend to parallel the bilayer normal. However, these values are small and many negative values are present in the plots. This indicates that on average, the drugs are tilted with respect to the bilayer normal. Such an orientation was also found by Stouch et al. in a simulation of a drug analogue in a DMPC bilayer [18], and also agrees with the behaviour observed for the drug head reported earlier. The same explanation may apply for the drug vector: the molecules orient themselves in the membrane to optimize their H-bonds.

Considering P_2 and P_1 plots together, the conclusions are: drugs are mainly tilted with respect to the bilayer normal, up→down and down→up interconversions are possible, and the preferred drug orientation is such as to maximise the number of H-bonds.

3.5. Orientational times

The ability of the small organic compounds to rotate around their centre of mass at different depths in the membrane was measured from the time autocorrelation function of the vector along the normal to the molecular plane. This is the same vector which was used in the previous section to calculate the angle θ with the bilayer normal and finally the order parameter S (Eq. (1)). The reorientational times for the β-blockers were studied by investigating two types of motions: those of the aromatic ring representing the drug head and those of the drug vector representing the overall drug orientation. Since the drug models were fully flexible, these two motions are in principle independent.

3.5.1. Small solute orientational times

The following time autocorrelation functions were studied:

$$C(t) = \left\langle P_2\left[\vec{\mu}(t)\cdot\vec{\mu}(0)\right]\right\rangle \quad (2)$$

P_2 is the Legendre polynomial of rank 2 and $\vec{\mu}$ is the unit vector along the normal to the molecular plane as defined previously to calculate the angle θ with the bilayer normal (see Section 3.4.1). The equation turns into:

$$C(t) = \frac{1}{2}\langle 3\cos^2\alpha - 1\rangle \quad (3)$$

where α is the change in angle between $\vec{\mu}$ at time t and at time 0. The resulting time autocorrelation functions were then fitted with single exponentials of form:

$$C(t) = C(0)\exp(-t/\tau) \quad (4)$$

From the fitting, the relaxation times, τ, for solute reorientation were obtained and plotted in Fig. 18. A general trend is observed: as expected, τ increases entering the membrane and reaches its highest values in regions 2 and 3, the densest parts of the bilayer. Benzene has the highest values of τ, since it is the largest permeant and its rotations in the packed lipid environment are the most difficult. The standard errors in Fig. 18 were calculated from the differences of the five independent simulations from their average. This shows that for the longest τs, the variability between the five simulations was the highest.

Benzene diffusion in the hydrocarbon region has been previously simulated by Stouch et al. [17]. Reorientational correlation times in that publication were found to be ≈25 ps. These simulations yield values of the same magnitude in region 4. However, in region 3 these simulations yield values 3 to 4 times higher. This is associated with the more restricted

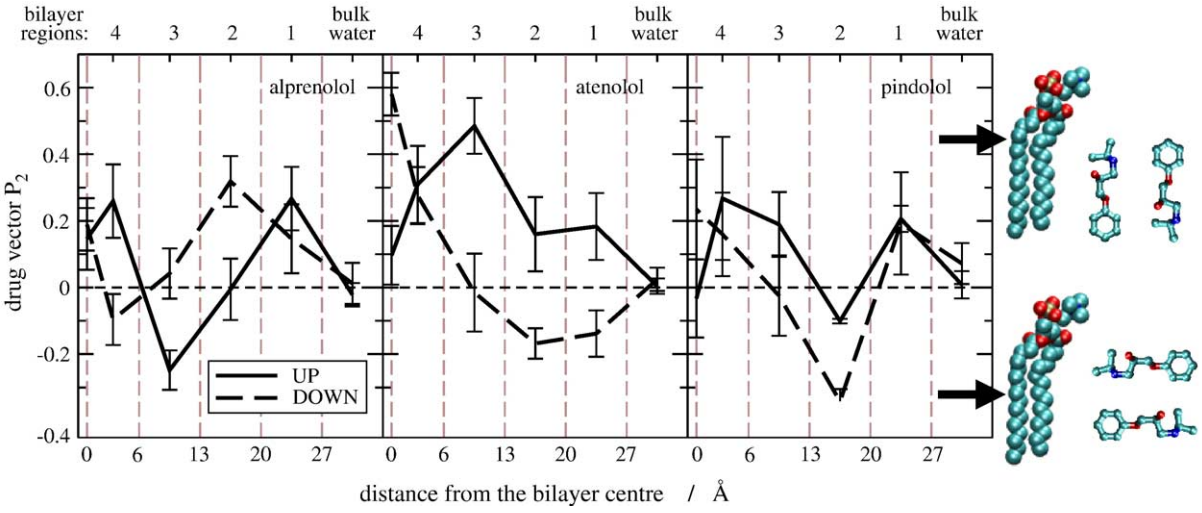

Fig. 17. The order parameter of the drug vector as a function of depth in the bilayer.

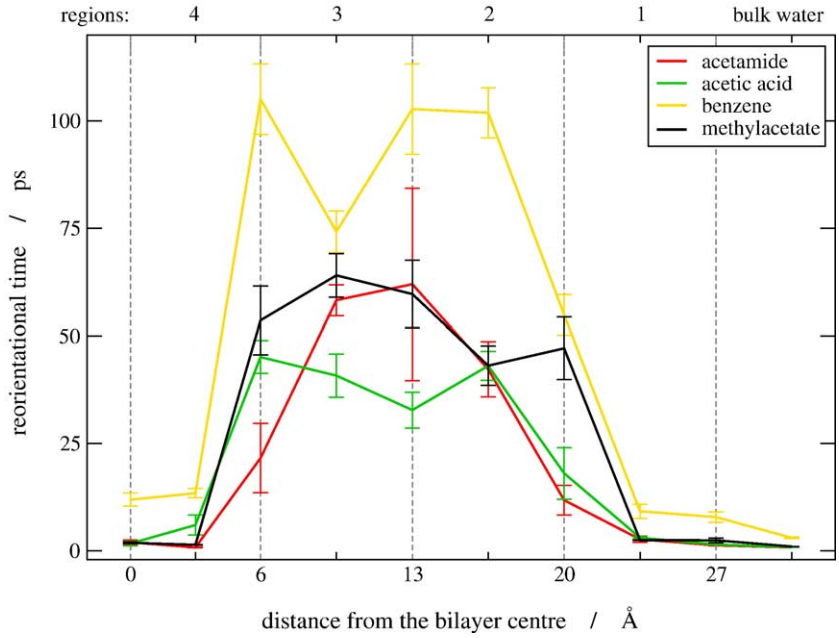

Fig. 18. Solute reorientational correlation times as a function of depth in the membrane.

benzene sampling observed in these studies, as explained in Section 3.4.1 regarding the differences in surface area and temperature between these and Stouch's simulations.

That inside the membrane orientational times are much longer than in water solution gives a molecular interpretation to explain the experimental observation that water/membrane partitioning is highly affected by entropic effects, as mentioned in the previous paper [4]: moving from water into the membrane does cause a loss of degrees of freedom for the permeant molecules. This is also consistent with the significantly lower partition coefficient of benzene in the middle of the lipid bilayer than in hexadecane, as shown in the previous papers [3,4]. It is also noted that correlation times for small solute reorientations inside the lipid bilayer are longer than the correlation times of the force instantaneous fluctuations employed in the calculation of diffusion coefficients [3,4].

3.5.2. Drug head orientational times

As previously mentioned, the drug head orientation was studied in terms of the angle between the normal to the aromatic ring plane and the bilayer normal. Time autocorrelation functions were constructed using Eqs. (2) and (3).

Time autocorrelation functions could be fitted with a double exponential for $z=30.5$ Å (i.e., when drugs are still in water), with two characteristic decay times τ_{long} and τ_{short}. Inside the membrane, triple exponentials were required for a complete description of these motions, with a third decay time τ_{flip}. Correlation coefficients were all higher than 0.97. The results for all drugs were very similar.

τ_{short} is between 0.5 and 5 ps and it corresponds to the oscillations of the aromatic ring around a stable orientation. τ_{long} is instead related to significant orientational changes and is between 10 and 100 ps. τ_{flip} is in the order of magnitude of several hundreds of ps and in some cases a few ns, even longer than the total simulation. This decay time is difficult to interpret, but it seems to be related to drastic changes such as the interconversion of drug orientation from up to down or vice versa. Probably, it is not the case that at $z=30.5$ Å τ_{flip} does not exist, but rather it is simply as fast as other motions and is hidden by, for instance, τ_{long}. If fitting is done with triple exponential at $z=30.5$ Å too, it is seen that indeed τ_{long} and τ_{flip} have similar values.

From these simulations, there is no direct correlation between location inside the membrane and decay times. This suggests that either the statistics are very poor, or that drug head motions have on average similar times at all depths. The first hypothesis could be true for τ_{flip}, since it is very long or even longer than the whole simulation, but is less likely for τ_{long} or τ_{short}.

3.5.3. Drug vector orientational times

The same time autocorrelation function was employed for studying the reorientational time of the drug vector. In this case, μ is the unit vector of the drug vector.

The same results obtained with the drug head were also obtained with the drug vector. Time autocorrelation functions could be fitted with a double exponential at $z=30.5$ Å, while they required triple exponentials inside the membrane. Similar values for the three decay times were found and they were related to the same type of motions. It seems then that drug head and vector are closely related, since their motions have identical characteristic times. Looking again at Fig. 5, it is easy to understand a possible reason for this behaviour. The picture shows the preferred drug configurations. It is

clear that the drug is preferentially elongated and any time its head changes orientation with respect to the bilayer normal the same change in orientation occurs for the drug vector, or vice versa. If one calculates the normalized time autocorrelation function of the difference between the angle formed by the drug head with the bilayer normal and the angle formed by the drug vector with the bilayer normal, at $z = 30.5$ Å, a decay time around 50 ps is obtained, but in the membrane interior it is in the ns time scale. This confirms that the two molecular fragments have correlated motions in the membrane interior.

As for the small organic solutes, for the larger drug molecules it appears that the correlation times for reorientational changes inside the membrane are much longer than the correlation times of the force fluctuations employed in the calculation of diffusion coefficients [5]. Consequently, the two types of correlation times must reflect two different and uncoupled types of motion.

4. Conclusions

In this paper, the atomic behaviour inside a phospholipid bilayer was investigated for small organic solutes and three drugs belonging to the class of β-adrenoreceptors antagonists by means of MD simulations.

Despite their differences in size, all the small organic compounds, to a greater or lesser extent, tend to permeate the lipid bilayer with a preferred orientation parallel to the bilayer normal, above all in the densest part of the membrane. Polar groups are preferentially oriented towards the lipid headgroups, where they can be involved in hydrogen-bonds. Hydration has also been observed in the middle of the membrane, which is usually considered an almost completely hydrophobic environment.

Inside the membrane, both the drug head and the drug tail tend to stay parallel to the lipid molecules. However, perpendicular orientations and up → down and down → up interconversions do occur during the simulations to make possible the formation of H-bonds between both the drug tail and the drug side chain with the surrounding lipids and waters. Isotropic motions are observed in the water phase. In the membrane interior, however, correlation times for drug reorientation are of the order of a few ns. From these simulations, hydrogen bonding possibilities seem to be as important as steric constraints in determining the drug behaviour inside the membrane. The importance of H-bonds is recognised in drug design to be one of the most critical factor affecting drug absorption [40].

Analysis of dihedral torsions shows that the drugs tend to stay elongated inside the lipid bilayer. Only at the very end of the drug tail is there significant variation, with the drugs staying more folded closer to the interface, or more stretched closer to the bilayer centre. This has important consequences for the intramolecular hydrogen bonds, with different pairs of functional groups involved depending on the drug conformation. The preference for the drug to stay elongated also makes the motions of its head (an aromatic ring) and its tail (a hydrocarbon chain) strongly correlated and with similar decay times. Simulations starting with different dihedral angle values yield at the end similar populations, suggesting that a few ns of simulation gives reliable sampling of the drugs' internal degrees of freedom. This work also shows that implicit solvent studies as used here, and presented elsewhere [5], are not required to select drug conformers, and that they are not able to yield the correct angle distributions in the condensed phase.

During the submission of this manuscript, a similar work was published by Tieleman et al. [41]. There, no free energies, diffusion coefficients or permeability coefficients were calculated, but instead the distribution of pentachlorophenol inside two different unsaturated lipid bilayers was obtained by standard molecular dynamics simulations. By allowing the simulations run for 25–35 ns, different starting distributions of pentachlorophenol inside and outside the membrane converged to essentially the same distribution, which then was stable over another 15–25 ns. The solute (a biopollutant) preferentially occupied the region between the carbonyl groups and the double bonds in the acyl chains. In agreement with the findings from our simulations, pentachlorophenol tended to be aligned parallel to the bilayer normal, formed H-bonds with surrounding lipids and water molecules, and entropy opposed its water/membrane partitioning. Even though the solute was in high concentration, the effect on lipid order parameters and bilayer thickness was small, but the tilt of lipid molecules decreased.

A comment is required regarding the use of a temperature of 50 °C for these simulations. This temperature is necessary for DPPC bilayers to be in the liquid crystal and biologically relevant Lα phase. Although human cells and cells of other important organisms live at lower temperatures, they too are in the Lα phase, and the model membrane must reflect this.

It should be noted that the present study has only targeted a pure DPPC bilayer, whereas biological membranes contain different lipid molecules and proteins. These simulations are certainly a step forward to investigate the atomic detail of drug membrane permeation and the next step would be to include a different membrane model, together with different drug permeants. Comments on the effects on the overall permeability coefficients caused by more complex membranes are reported elsewhere [5]. Effects at the molecular level are more difficult to predict. How the presence of different lipids or proteins would change for example the solute orientation or hydrogen bonding patterns is difficult to infer and would be mainly speculation. For instance, if the different lipid and protein composition causes a higher distribution of free volume, the permeant molecules would have a higher orientational freedom and disorder, thus reducing the entropy cost of water/membrane partitioning and increasing the diffusion coefficients. If the membrane components are more polar or have more hydrogen bonding groups, polar permeants and hydrogen bonding solutes

would partition more favourably, but would perhaps have lower diffusion coefficients because of the stronger interactions with the membrane. Results from this work suggest that MD simulations of drugs in membranes can help to rationalise the experimental permeation process in terms of detailed intermolecular interactions. Although these simulations are not suitable yet for high-through-put screening, this approach can in principle be associated with rational drug design, given that computer power is continuously increasing.

Acknowledgements

We would like to thank the EPSRC and Aventis for funding the project. Also thanks to I.C. Walton, I.D. Hardy and O.G. Parchment for their help in running the simulations on the Southampton University PC cluster called IRIDIS (http://www.sucs.soton.ac.uk/research/iridis/).

References

[1] S. Balaz, Lipophilicity in trans-bilayer transport and subcellular pharmacokinetics, Perspect. Drug Discov. Des. 19 (2000) 157–177.
[2] S. Singer, G.L. Nicolson, The fluid mosaic model of cell membranes, Science 172 (1972) 720–730.
[3] D. Bemporad, J.W. Essex, C. Luttmann, Permeation of small molecules through a lipid bilayer: a computer simulation study, J. Phys. Chem., B 108 (2004) 4875–4884.
[4] D. Bemporad, J.W. Essex, C. Luttmann, Computer simulation of small molecule permeation across a lipid bilayer: dependence on bilayer properties and solute volume, size and cross-sectional area, Biophys. J. 87 (2004) 1–13.
[5] D. Bemporad, Computer simulation of biological membranes and small molecule permeation, Ph.D. thesis, University of Southampton, Southampton (January 2003).
[6] A.D. MacKerell, S.E. Feller, An improved empirical potential energy function for molecular simulations of phospholipids, J. Phys. Chem., B 104 (2000) 7510–7515.
[7] S.E. Feller, R.M. Venable, R.W. Pastor, Computer simulation of a dppc phospholipid bilayer: structural changes as a function of molecular surface area, Langmuir 13 (1997) 6555–6561.
[8] J.P. Ryckaert, G. Ciccotti, H.J.C. Berendsen, Numerical integration of the cartesian equations of motion of a system with constraints: molecular dynamics of n-alkanes, J. Comp. Phys. 23 (1977) 327–341.
[9] R.W. Hockney, The potential calculation and some applications, Methods Comput. Phys. 9 (1970) 136–211.
[10] S.E. Feller, Y. Zhang, R.W. Pastor, B.R. Brooks, Constant pressure molecular dynamics simulation: the Langevin piston, J. Chem. Phys. 103 (1995) 4613–4621.
[11] W.G. Hoover, Canonical dynamics: equilibrium phase-space distributions, Phys. Rev., A 31 (1985) 1695–1697.
[12] H.J.C. Berendsen, S.J. Marrink, Molecular dynamics of water transport through membranes: water from solvent to solute, Pure Appl. Chem. 65 (1993) 2513–2520.
[13] S.J. Marrink, H.J.C. Berendsen, Simulation of water transport through a lipid-membrane, J. Phys. Chem. 98 (1994) 4155–4168.
[14] S.J. Marrink, H.J.C. Berendsen, Permeation process of small molecules across lipid membranes studied by molecular dynamics simulations, J. Phys. Chem. 100 (1996) 16729–16738.
[15] B.R. Brooks, R.E. Bruccoleri, B.D. Olafson, D.J. States, S. Swaminathan, M. Karplus, Charmm—A program for macromolecular energy, minimization, and dynamics calculations, J. Comput. Chem. 4 (1983) 187–217.
[16] K. Tu, M. Tarek, M.L. Klein, D. Scharf, Effects of anesthetics on the structure of a phospholipid bilayer: molecular dynamics investigation of halothane in the hydrated liquid crystal phase of dipalmitoylphosphatidylcholine, Biophys. J. 75 (1998) 2123–2134.
[17] D. Bassolino-Klimas, H.E. Alper, T.R. Stouch, Solute diffusion in lipid bilayer-membranes—an atomic-level study by molecular–dynamics simulation, Biochemistry 32 (1993) 12624–12637.
[18] H.E. Alper, T.R. Stouch, Orientation and diffusion of a drug analog in biomembranes–molecular–dynamics simulations, J. Phys. Chem. 99 (1995) 5724–5731.
[19] K. Palm, K. Luthman, A.L. Ungell, G. Strandlund, P. Artursson, Correlation of drug absorption with molecular surface properties, J. Pharm. Sci. 85 (1996) 32–39.
[20] K. Palm, K. Luthman, A.L. Ungell, G. Strandlund, F. Beigi, P. Lundahl, P. Artursson, Evaluation of dynamic polar molecular surface area as predictor of drug absorption: comparison with other computational and experimental predictors, J. Med. Chem. 41 (1998) 5382–5392.
[21] M. Pasenkiewiczgierula, Y. Takaoka, H. Miyagawa, K. Kitamura, A. Kusumi, Hydrogen bonding of water to phosphatidylcholine in the membrane as studied by a molecular dynamics simulation: location, geometry, and lipid–lipid bridging via hydrogen-bonded water, J. Phys. Chem., A 101 (1997) 3677–3691.
[22] J. Ulander, A.D.J. Haymet, Permeation across hydrated dppc lipid bilayers: simulation of the titrable amphiphilic drug valproic acid, Biophys. J. 85 (2003) 3475–3484.
[23] A. Grossfield, T.B. Woolf, Interaction of tryptophan analogs with popc lipid bilayers investigated by molecular dynamics calculations, Langmuir 18 (2002) 198–210.
[24] D. Bassolino-Klimas, H.E. Alper, T.R. Stouch, Mechanism of solute diffusion through lipid bilayer-membranes by molecular–dynamics simulation, J. Am. Chem. Soc. 117 (1995) 4118–4129.
[25] T.R. Stouch, H.E. Alper, D. Bassolino, Simulations of drug diffusion in biomembranes, Comput.-Aided Mol. Des. 589 (1995) 127–138.
[26] G. Cevc, D. Marsh, Phospholipid Bilayers. Physical Principles and Models, John Wiley and Sons, New York, 1987.
[27] S.A. Simon, W.L. Stone, P. Busto-Latorre, A thermodynamic study of the partition of n-hexane into phosphatidylcholine and phosphatidylcholine-cholesterol bilayers, Biochim. Biophys. Acta 468 (1977) 378–388.
[28] T.J. McIntosh, S.A. Simon, R.C. MacDonald, The organization of n-hexanes in lipid bilayers, Biochim. Biophys. Acta 597 (1980) 445–463.
[29] R.A. Badley, W.G. Martin, H. Schneider, Dynamics behaviour of fluorescent probes in lipid bilayer model membranes, Biochemistry 12 (1973) 268–275.
[30] J. Frenzel, K. Arnold, P. Nuhn, Calorimetric, ^{13}c nmr, and ^{31}p nmr studies on the interaction of some phenothiazine derivatives with dipalmitoylphosphatidylcholine model membranes, Biochim. Biophys. Acta 507 (1978) 185–197.
[31] L.G. Herbette, A.M. Katz, J.M. Sturtevant, Comparisons of the interaction of propranolol and timolol with model and biological membrane systems, Mol. Pharmacol. 24 (1983) 259–269.
[32] Y. Boulanger, S. Schreier, I.C.P. Smith, Molecular details of anesthetic-lipid interactions as seen by deterium and phosphorus-31 nuclear magnetic resonance, Biochemistry 20 (1981) 6824–6830.
[33] D.G. Rhodes, J.G. Sarmiento, L.G. Herbette, Kinetics of binding of membrane-active drugs to receptor sites, Mol. Pharmacol. 27 (1985) 612–623.
[34] L.R. De Young, K.A. Dill, Solute partitioning into lipid bilayer membranes, Biochemistry 27 (1988) 5281–5289.
[35] L.R. De Young, K.A. Dill, Partitioning of nonpolar solutes into bilayers and amorphous n-alkanes, J. Phys. Chem. 94 (1990) 801–809.

[36] T.X. Xiang, X. Chen, B.D. Anderson, Transport methods for probing the barrier domain of lipid bilayer membranes, Biophys. J. 63 (1992) 78–88.
[37] T.X. Xiang, B.D. Anderson, Phospholipid surface density determines the partitioning and permeability of acetic acid in dmpc:cholesterol bilayers, J. Membr. Biol. 148 (1995) 157–167.
[38] T.X. Xiang, B.D. Anderson, Permeability of acetic acid across gel and liquid-crystalline lipid bilayers conforms to free-surface-area theory, Biophys. J. 72 (1997) 223–237.
[39] L.G. Herbette, D.W. Chester, D.G. Rhodes, Structural analysis of drug molecules in biological membranes, Biophys. J. 49 (1986) 91–94.
[40] C.A. Lipinski, F. Lombardo, B.W. Domony, P.J. Feeney, Experimental and computational approaches to estimate solubility and permeability in drug discovery and development settings, Adv. Drug Deliv. Rev. 23 (1997) 3–25.
[41] P. Mukhopadhyay, H.J. Vogel, D.P. Tieleman, Distribution of pentachlorophenol in phospholipid bilayers: a molecular dynamics study, Biophys. J. 86 (2004) 337–345.